arXiv:1511.09195v1 [cond-mat.mtrl-sci] 30 Nov 2015

Strong charge and spin fluctuations in $La_2O_3Fe_2Se_2$

Guangxi Jin,[1,2] Yilin Wang,[3] Xi Dai,[3] Xinguo Ren,[1,2] and Lixin He[1,2]

[1]*Key Laboratory of Quantum Information, University of Science and Technology of China, Hefei, 230026, China*
[2]*Synergetic Innovation Center of Quantum Information and Quantum Physics, University of Science and Technology of China, Hefei, 230026, China*
[3]*Beijing National Laboratory for Condensed Matter Physics, and Institute of Physics, Chinese Academy of Sciences, Beijing 100190, China*

(Dated: December 1, 2015)

The electronic structure and magnetic properties of the strongly correlated material $La_2O_3Fe_2Se_2$ are studied by using both the density function theory plus U (DFT+U) method and the DFT plus Gutzwiller (DFT+G) variational method. The ground-state magnetic structure of this material obtained with DFT+U is consistent with recent experiments, but its band gap is significantly overestimated by DFT+U, even with a small Hubbard U value. In contrast, the DFT+G method yields a band gap of 0.1 - 0.2 eV, in excellent agreement with experiment. Detailed analysis shows that the electronic and magnetic properties of of $La_2O_3Fe_2Se_2$ are strongly affected by charge and spin fluctuations which are missing in the DFT+U method.

PACS numbers: 71.20.-b, 71.27.+a, 75.30.-m,

I. INTRODUCTION

Because of their close relationship with the Fe-based high-T_c superconductor, there has been revived interest in iron oxychalcogenides, $R_2O_3T_2X_2$ (R=rare earth element, T=transition metal element, X=S or Se), which have similar crystal structures.[1,2] One example is $La_2O_3Fe_2Se_2$ (LOFS), which was first explored by Mayer et al.,[3] and considered to be a strongly correlated material composed of the transition metal ion Fe^{2+}. Analogous to its oxychalcogenides relatives, LOFS was determined to be a semiconductor by experiment and claimed to be a Mott insulator.[2]

The crystal structure of LOFS, with space group I4/mmm (No.139), is shown in Fig. 1. It is composed of alternating layered units of $[La_2O_2]^{2+}$ and $[Fe_2OSe_2]^{2-}$, stacking along the c-axis. The layered sheets of $[La_2O_2]^{2+}$, formed by edge-sharing La_4O tetrahedra, expand along the a-b plane. The $[Fe_2OSe_2]^{2-}$ layers consist of face-sharing FeO_2Se_4 octahedra, where the Fe atom is surrounded by two axial oxygen atoms and four equatorial selenium atoms, forming a tilted Fe-centered octahedron with the D_{2h} point symmetry. Viewed along the c-axis, the Fe atoms in $[Fe_2OSe_2]^{2-}$ layer form checkerboard lattice, and the Fe-Fe interactions are mediated by Fe-O-Fe and Fe-Se-Fe bonds.

Despite of the considerable research in the past, there are still some mysteries about this material to be understood. First, the magnetic structure of LOFS was found to be anti-ferromagnetic(AFM) below the critical temperature $T_N \sim 90$ K. However, two possible magnetic ground states have been proposed by experiments. The first model (Model I) was proposed in Ref. 2. Within this model, the AFM ground state is described by the propagation vector $\mathbf{k}$=(0.5, 0, 0.5), and the Fe ions form a spin-frustrated magnetic structure, which align ferromagnetially along the a-axis and antiferromagnetially along the b-axis.[2,4] An interesting aspect of this magnetic structure is that it lacks inversion symmetry, which may further break the inversion symmetry of the crystal, resulting in ferroelectricity by the exchange-striction effect as possible magnetic ferroelectrics.[5,6] The second model (Model II) is a non-collinear AFM model, which is composed of two magnetic sublattices with propagation vectors $\mathbf{k}_1 = (0.5, 0, 0.5)$ and $\mathbf{k}_2 = (0, 0.5, 0.5)$, respectively. This magnetic structure was first proposed by Fuwa et. al.[7] for $Nd_2O_3Fe_2Se_2$ and was identified as the magnetic structure for LOFS by recent experiments.[8,9] Within this model, the spins align in parallel in each sublattice, and perpendicular between different sublattice. In contrast with Model I, the magnetic structure of Model II still possesses the inversion symmetry.

Second, the magnitude of the local magnetic moment measured by different experiments scatters significantly, ranging from 2.62 μ_B to 3.50 μ_B.[2,4,8,9] Thus information from reliable first-principles calculations will be helpful to clarify the sitution.

Third, LOFS was determined to be a semiconductor by electrical resistivity measurement, with a small band gap of 0.17-0.19 eV.[1,4,10] However, the band gaps obtained by the DFT+U method, even for very small Hubbard U parameters, are significantly larger than the experimental values. This suggests that the Hartree-Fock type treatment of electron correlations, which neglects the multiplet effects, might not be sufficient for this system.

In this paper, we first identify the ground-state magnetic structure of LOFS via first-principles calculations. We calculated the total energies of different magnetic structures using density-functional theory (DFT), with on-site Coulomb interaction correction (DFT+U), including the two experimentally proposed magnetic structure models. Our results suggest that Model II is the ground state-magnetic structure of LOFS. However, the DFT+U method greatly overestimates the band gap of LOFS.[11] In order to correctly describe the electronic structure of LOFS,[1,10] we further calculated the elec-

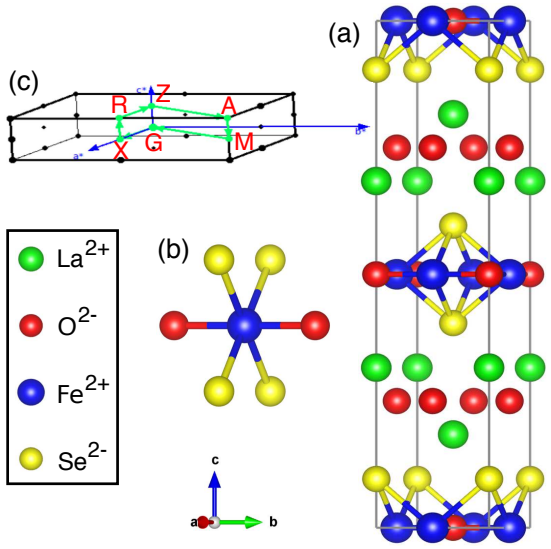

FIG. 1: (a). Crystal structure of LOFS, where green, red, blue and yellow balls represent La^{3+}, O^{2-}, Fe^{2+} and Se^{2-}, respectively; (b) FeO_2Se_4 octahedra, where the Fe atom is surrounded by two axial oxide ions and four equatorial selenide ions, forming a tilted Fe-centered octahedron with the D_{2h} point symmetry (c) Symmetry points in the Brillouin zone.

tronic and magnetic properties of this compound by the DFT plus Gutzwiller (DFT+G) method. With appropriate U, J, parameters, the obtained DFT+G band gap is approximately 0.1 eV - 0.2 eV, in excellent agreement with experiment. The local magnetic moment obtained by DFT+G is about 3.0 μ_B, falling within the range of experimental results, but is somewhat smaller than the DFT+U values, which are approximately 3.4 - 3.6 μ_B. Detailed analysis shows that there are strong charge and spin fluctuations in this system, which are responsible for a significant reduction of the band gap.

The rest of the paper is organized as follows. In Sec.II, the methods used in our calculations are described. In Sec. III A, we determine the ground-state magnetic structure of LOFS by comparing the total energies of various spin configurations using DFT+U method. In Sec. III B, we study its band structure using DFT+G method. A summary of our work is given in Sec: IV.

II. COMPUTATIONAL DETAILS

A. DFT+U

We perform first-principles calculations based on DFT within the spin-polarized generalized gradient approximation (SGGA) using Perdew-Burke-Ernzerhof functional,[12] implemented in the Vienna ab initio simulations package (VASP).[13,14] The projector-augmented-wave (PAW) pseudopotentials with a 500 eV plane-wave cutoff are used. To account for the correlation effect of Fe ions, we add on-site Coulomb interaction U as is done in the DFT+U scheme.[15] The total energies are converged to 10^{-8} eV.

B. DFT+G

LOFS is a strongly correlated system, whose band structure understandably cannot be well described by single-particle mean-field approximations like DFT+U. As mentioned above and detailed below, the band gap obtained from DFT+U calculations are too big. To correct this, we resort to the DFT+G variational method,[16,17] which can treat the multiplet effects more accurately. The DFT+G method starts with the following many-body Hamiltonian,

$$\begin{aligned}\hat{H} =&\hat{H}_{TB} + \hat{H}_{int} + \hat{H}_{dc} \\ =&\hat{H}_{TB} + \sum_i \hat{H}_{i,atom} - \sum_i \hat{H}_{i,dc}\,.\end{aligned} \tag{1}$$

The first term in Eq. (1) is a d-p tight-binding (TB) Hamiltonian constructed from non-spin-polarized GGA band structure, projected to the d-p manifold of maximally localized Wannier functions.[18–21] This term apparently describes the hopping of electrons. The Wannier functions contains not only the localized $3d$ orbitals of Fe atoms, but also extended $2p$ orbitals of O atoms and $4p$ orbitals of Se atoms. Using the Wannier functions, the TB term can be written more explicitly as,

$$\begin{aligned}\hat{H}_{TB} = &\sum_{\substack{i,j\\ m_1,m_2\\ \sigma}} t_{i,j}^{m_1\sigma,m_2\sigma}\hat{d}^\dagger_{im_1\sigma}\hat{d}_{jm_2\sigma} + \sum_{\substack{i,j\\ m_1,m_2\\ \sigma}} t_{i,j}^{m_1\sigma,m_2\sigma}\hat{p}^\dagger_{im_1\sigma}\hat{p}_{jm_2\sigma} \\ &+ \sum_{\substack{i,j\\ m_1,m_2\\ \sigma}} t_{i,j}^{m_1\sigma,m_2\sigma}\hat{d}^\dagger_{im_1\sigma}\hat{p}_{jm_2\sigma} + \sum_{\substack{i,j\\ m_1,m_2\\ \sigma}} t_{i,j}^{m_1\sigma,m_2\sigma}\hat{p}^\dagger_{im_1\sigma}\hat{d}_{jm_2\sigma}\end{aligned} \tag{2}$$

where the operator $\hat{d}^\dagger_{im\sigma}(\hat{d}_{im\sigma})$ creates (annihilates) a $3d$ electron of Fe atom on site i, with orbital m and spin σ. Likewise, $\hat{p}^\dagger_{im\sigma}(\hat{p}_{im\sigma})$ creates (annihilates) a p electron of O and Se atoms.

The second term in Eq. (1) is a rotationally invariant Coulomb interaction Hamiltonian describing the strong on-site electron-electron interactions within the $3d$ orbitals of Fe atoms. We assume the spherical symmetry of local environment of the Fe atom and use a full interaction tensor as $U_{m_1\sigma,m_2\sigma',m_3\sigma',m_4\sigma}$. For the detailed definition of the U tensor, we follow the method described in Ref. 22. Within the complex spherical harmonics basis, the second term of the Hamiltonian in Eq. (1) can be explicitly expressed as,[23]

$$\begin{aligned}&\hat{H}_{i,atom} \\ =&\sum_{\substack{m_1,m_2,m_3,m_4\\ \sigma,\sigma'}} U_{m_1\sigma,m_2\sigma',m_3\sigma',m_4\sigma}\hat{d}^\dagger_{m_1\sigma}\hat{d}^\dagger_{m_2\sigma'}\hat{d}_{m_3\sigma'}\hat{d}_{m_4\sigma}\end{aligned} \tag{3}$$

where the U tensor satisfies the condition,

$$U_{m_1\sigma,m_2\sigma',m_3\sigma',m_4\sigma} = \delta_{m_1+m_2,m_3+m_4} \sum_k c_k^{m_1,m_4} c_k^{m_2,m_3} F^k \,. \tag{4}$$

Here, m_1, m_2, m_3 and m_4 are the orbital index, σ, σ' denote the spin states, $c_k^{m_1,m_4}$ are the Gaunt coefficients, and F^k is the Slater integrals. For the d shell, k=0, 2, 4, and hence the full U tensor can be specified by the parameters F^0, F^2 and F^4. According to Wang et. al.,[22] $F^4/F^2 = 0.625$ is an approximation with good accuracy for the d shell,[24] and hence is also adopted in this work. The intra-orbital Coulomb interaction and Hund's rule coupling are set to be $U = F^0 + \frac{4}{49}F^2 + \frac{4}{49}F^4$, and $J = \frac{5}{98}(F^2 + F^4)$, respectively. Therefore, given the parameter values of either F^0, F^2 or U, J, we can construct the full interaction U tensor.

The last term of Eq. (1) is a double-counting (DC) term in order to substrate the correlation effect which has been partially included in DFT calculations. The DC term is not uniquely defined, and here we adopted the choice used in Ref. 25, where it can be expressed as

$$\begin{aligned} \hat{H}_{dc} &= \sum_\sigma U_{dc}^\sigma \hat{n}_d^\sigma \\ U_{dc}^\sigma &= U(n_d - \frac{1}{2}) - J(n_d^\sigma - 1)/2 \\ n_d^\sigma &= \sum_m \langle \Psi_G | \hat{d}_{m\sigma}^\dagger \hat{d}_{m\sigma} | \Psi_G \rangle \,. \end{aligned} \tag{5}$$

The Gutzwiller trial wave function $|\Psi_G\rangle$ is constructed by applying a projection operator $\hat{P}$ on the uncorrelated wave function $|\Psi_0\rangle$ from DFT calculations,

$$|\Psi_G\rangle = \hat{P}|\Psi_0\rangle \tag{6}$$

with

$$\hat{P} = \prod_{\mathbf{R}} \hat{P}_{\mathbf{R}} = \prod_{\mathbf{R}} \sum_{\Gamma,\Gamma'} \lambda(\mathbf{R})_{\Gamma\Gamma'} |\Gamma, \mathbf{R}\rangle\langle\Gamma', \mathbf{R}| \tag{7}$$

where $|\Gamma, \mathbf{R}\rangle$ are the eigenstates of the on-site Hamiltonian $\hat{H}_{i,atom}$ for site $\mathbf{R}$, and $\lambda(\mathbf{R})_{\Gamma\Gamma'}$ are the Gutzwiller variational parameters to be determined by minimizing the total-energy of the ground state $|\Psi_G\rangle$, through the variational method.[16,17] More details of this method can be found in Refs. 17 and 26.

III. RESULTS AND DISCUSSION

In this section, we first study the magnetic ground state of LOFS using the DFT+U method. The most stable magnetic configuration coming out from our DFT+U calculations agrees with the one proposed by Fuwa and coworkers.[7] However, as mentioned above, the DFT+U method significantly overestimates the band gap of LOFS. We then study the band structure of LOFS using the DFT+G method.

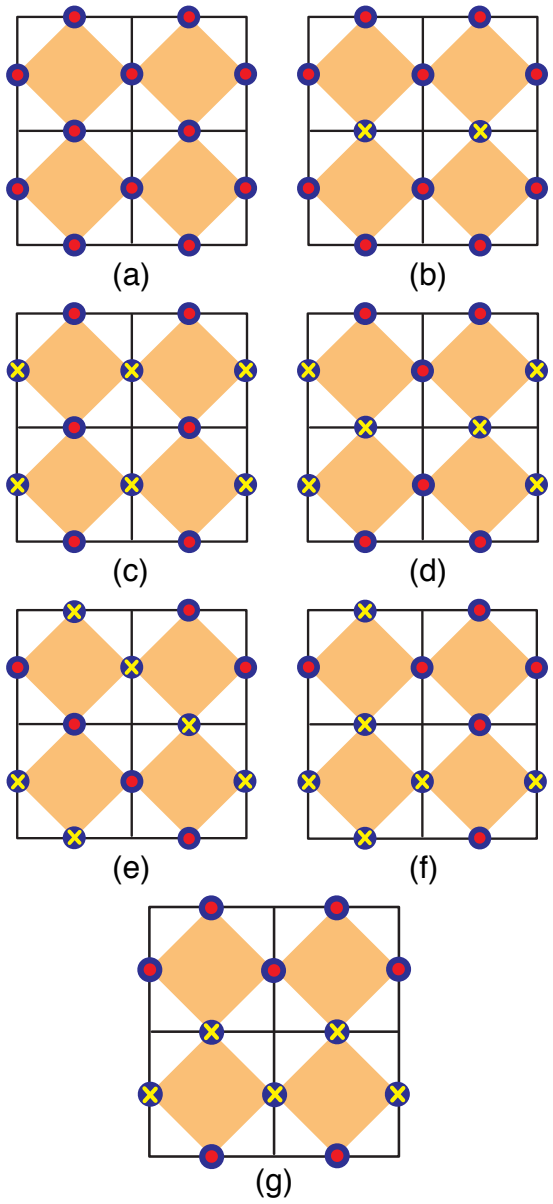

FIG. 2: (a)-(g) The magnetic structures of one layer of Fe atoms in the crystalline ab plane. Only the Fe atoms are shown in figures, which is indicated by large blue circles; and the small red circle and yellow cross represent up and down spin orientation, respectively.

A. Results from DFT+U

In order to identify the magnetic structure of the ground state, we performed a series of DFT+U total energy calculations for different magnetic configurations. In LOFS, each unit cell contains two $[Fe_2OSe_2]^{2-}$ layers along the c-axis. Atomic positions of the second $[Fe_2OSe_2]^{2-}$ layer are shifted by (0.25, 0.25, 0.25) of the lattice vectors relative to the first layer. Possible magnetic configurations in each layer are shown in Fig. 2. The magnetic structures in a unit cell are then the combina-

tions of the magnetic configurations of the two layers. For example the configuration [(b)+(a)] means the first layer takes configuration (b), whereas the second layer takes configuration (a). This notational system is similar to that used by Zhu et. al.[1] and Zhao et. al.[11]

We calculated the total energies of seven magnetic structures, including (1) FM[(a)+(a)], (2) AFM1[(c)+(c)], (3) AFM2[(b)+(a)], (4) AFM3[(g)+(g)], (5) AFM4[(d)+(f)], (6) AFM5[(e)+(e)], (7) AFM6[(d)+(d)]. In the AFM3 configuration, the spins in each $[Fe_2OSe_2]^{2-}$ layer form a double stripe AFM structure along the a-axis,[2], which is different from the structure used in Ref. 1 and Ref. 11. AFM3 is actually the experimental magnetic structure Model I proposed by Free et. al.,[2] whereas the AFM6 configuration corresponds to the experimental magnetic model II, within the collinear approximation. Such an approximation was previously adopted for $Sr_2F_2Fe_2OS_2$ in Ref. 11, because the magnetic-anisotropy energies are rather small compared to the energy differences between different configurations (see below).

Experimentally it was found that the spins form AFM along the c-axis. We calculate the total energy of spin configurations with propagation vectors (1/2,0,1/2) and (1/2,0,0) for the experimental magnetic model I (AFM3, using a 2×1×2 supercell. We found that the energy difference between the AFM spin configuration along the c-axis with magnetic propagation vector $\mathbf{k}$=(0.5, 0, 0.5), and the ferromagnetic configuration along c-axis with propagation vector $\mathbf{k}$=(0.5, 0, 0), is only about 0.1 meV in a 2×1×2 sueprcell. Therefore, in the following studies, we ignore the anti-ferromagnetic configuration between the unit cells along the c-axis, and focus on the magnetic structure in the ab plane. To accommodate all seven magnetic structures, we use a 2×2×1 supercell. The corresponding Monkhorst k-mesh is set to 8×8×4.

The calculated energies for different magnetic configurations, are listed in Table I for various effective Coulomb U_{eff}=U-J, where U, and J are the Coulomb and Hund's exchange interactions respectively . One can see that, for all U_{eff}, the total energy of AFM6 is significantly lower than those of AFM3 and other spin configurations. The magnetic ground state of LOFS is then determined to be AFM6 for all the values of U_{eff} considered in our DFT+U calculations. We therefore conclude that the experimental magnetic structure Model II should be the ground state magnetic structure in LOFS. These results are consistent with previous DFT+U calculations for $Sr_2F_2Fe_2OS_2$.[11] We note however, in Ref. 1, the ground state of LOFS was determined to be AFM6 for U_{eff}=0, 1.5 and 3.0 eV, but changed to AFM1 at U_{eff}=4.5 eV.

For comparison, we also calculated the total energies of different magnetic configurations for $Pr_2O_3Fe_2Se_2$, which has the similar crystal structure as LOFS.[27] We found that its magnetic ground state is also AFM6 within the DFT+U approximation, the same as that of LOFS and $Sr_2F_2Fe_2OS_2$.[11] These results suggest that the Model II magnetic structure should be the common character for the oxychalcogenide materials $R_2O_3Fe_2Se_2$ (R=rare earth).

TABLE I: Relative energy ΔE (meV/unit cell) of different magnetic configurations and various parameter U_{eff} (unit in eV), with the reference energy of FM, where the crystal structure was constrained at I4/mmm space group symmetry.

U_{eff}	FM	AFM1	AFM2	AFM3	AFM4	AFM5	AFM6
0	0	159.65	15.67	-120.09	-40.61	-10.04	-128.78
1.5	0	-237.42	-52.06	-237.12	-236.51	-341.42	-394.25
3.0	0	-220.76	-49.52	-194.86	-194.88	-273.04	-303.11
4.5	0	-184.12	-42.42	-148.38	-148.49	-201.93	-219.38

TABLE II: Magnetic moment (magmom) of LOFS, calculated by DFT+U method, under AFM6 magnetic configuration with different U_{eff}.

U_{eff} (eV)	0	1.5	3.0	4.5
magmom(μ_B)	-	3.4	3.5	3.6

After determining the ground-state magnetic structure, we calculate the magnetic moments of LOFS in the AFM6 configuration for different values of U_{eff}. The results are listed in Table II. The calculated magnetic moments of the Fe ion for different U_{eff} values are around 3.4 μ_B - 3.6 μ_B, which are in agreement with the experimental result 3.50 μ_B, obtained by McCabe et. al.[9]

To study the electronic structure of LOFS, we calculated the band structure and density of states (DOS) by using the DFT+U method for the AFM6 spin configuration, using different Coulomb U_{eff}=0 – 6.0 eV. The typical band structures of LOFS with U_{eff}=1.5 eV are shown in Fig. 3(a). Even for a small Coulomb U_{eff}=1.5 eV, the band gap is as large as 1.12 eV, which is significantly larger than the energy gap $E_g \sim$ 0.17 eV - 0.19 eV, extracted from the electrical resistivity measurement.[1,10] The calculated band gaps as a function of U are shown in Fig. 3(b). For U_{eff}=0, the system is metallic. For U_{eff} >0, there is a nearly linear dependence of the band gap upon the U_{eff} value as can be seen from Fig. 3(b). For a reasonable U_{eff}=4.5 eV, the calculated band gap is approximately 2.0 eV, which is about one order of magnitude larger than the experimental value. The results suggest that the correlation effects are not accounted for adequately by the DFT+U method, and more advanced methods are needed to describe the electronic structure of LOFS.

B. Results from DFT+G

To correctly describe the electronic structure of LOFS, we then performed DFT+G calculations under the ground state magnetic structure AFM6. We do calcu-

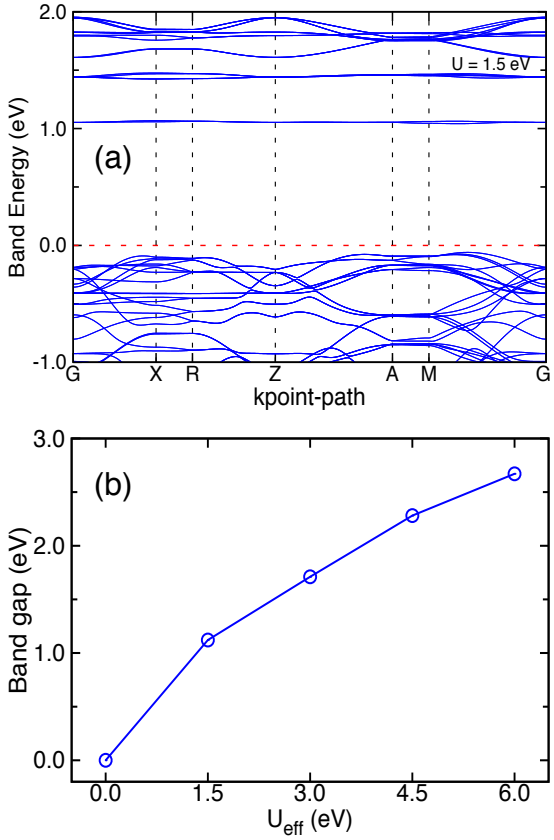

FIG. 3: (a) Band structure of LOFS calculated by DFT+U method, under the ground state magnetic structure AFM6 and U_{eff}=1.5 eV. The Fermi energy have been set to 0 eV. (b) The band gap of LOFS as a function of U_{eff} calculated by DFT+U method, under ground state magnetic structure.

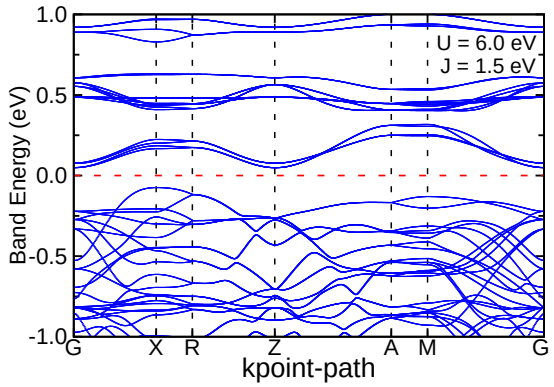

FIG. 4: Band structure of LOFS, calculated by DFT+G, with U=6.0 eV and J=0.25U, under ground state magnetic structure. The Fermi energy have been set to 0 eV.

lations with a series of Hubbard U=3.0 - 7.0 eV and Hund's exchange J=0.1 U - 0.3 U. We show the results here for typical parameters U=6.0 eV, J=0.25 U, which corresponds to U_{eff}=U-J=4.5 eV in the DFT+U calculations.

The band-structure calculated with typical U=6.0 eV and J=0.25 U is shown in Fig. 4. The DFT+G calculated band gap is approximately 0.121 eV, which is in excellent agreement with the value obtained by the electric resistivity measurement.[1,10] This is in stark contrast with those obtained from DFT+U calculations. For example, DFT+U gives a very large band gap (approximately 2.28 eV) with U_{eff}=4.5 eV. These results clearly demonstrate that the multiplets effects, which are missing in the DFT+U methods but captured in the DFT+G method, are crucial for a correct description of the electronic structure of LOFS.

We also calculate the magnetic moments of Fe atoms using the Gutzwiller wave functions. The magnetic moments of Fe atoms are approximately 3.08 μ_B for U=6.0 eV and J=0.25 U. This value is between the experimental results of Ref.[2] and Ref.[8], which are somehow smaller than those obtained from DFT+U calculations.

The differences between the DFT+U and DFT+G methods are that the DFT+G methods correctly take account of the multiplets effects whereas in DFT+U methods only a single atomic configuration is considered. To understand the results, we further analyzed the Gutzwiller wave functions. We calculated the probability of the atomic multiplets $|I\rangle$ of Fe atoms using the Gutzwiller ground state wave function $|G\rangle$, using the relation $P_I = \langle G|I\rangle\langle I|G\rangle$. To display the atomic configuration more explicitly, the crystal field splitting of Fe atom is shown in Fig. 5. The ten major atomic configurations with relatively large population are shown in Fig. 6(a), and corresponding populations are shown in Fig. 6(b) for U=6.0 eV, and J=0.25 U.

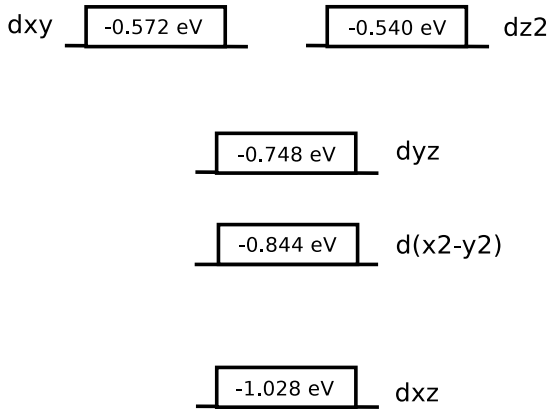

FIG. 5: Energy levels of Fe 3d states under crystal field splitting.

First we look at the electron occupation number of these atomic configurations. The atomic configurations cf1 has occupation number n=5 (yellow), and has the population P(n=5) = 0.015. Configurations cf2, cf3 have occupation number 6 (red), and their total population P(n=6) = 0.247. Configurations cf4, cf5, cf6, cf7, cf8 have occupation number 7 (blue) and total population P(n=7) = 0.4438, and configurations cf9, cf10 have occupation number 8 (green) with total population P(n=8)

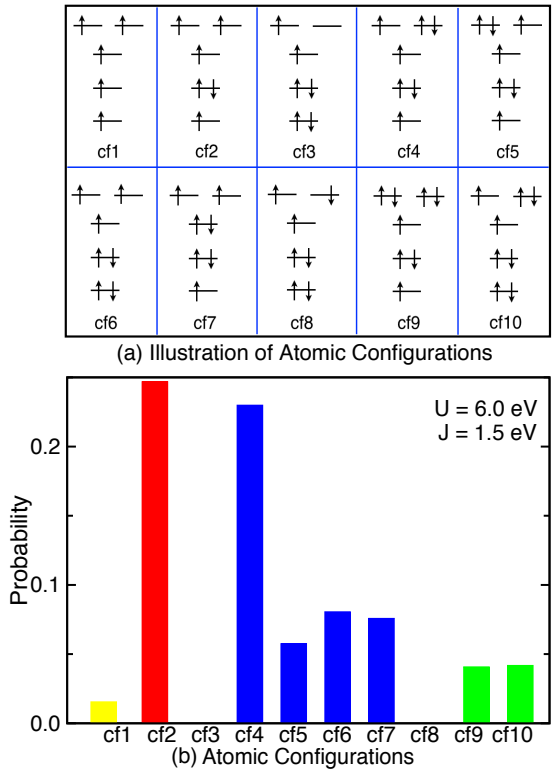

FIG. 6: (a) Illustration of main atomic configurations with relatively large probability; (b) Probability of the atomic configurations $|I\rangle$ in the Gutzwiller wave function $|G\rangle$, calculated with U=6.0 eV and J=0.25 U, under ground state magnetic structure. Here, the atomic configurations with occupation number 5, 6, 7 and 8, are represented by histograms with color yellow, red, blue and green, respectively.

= 0.0826. These results suggest that there are strong charge fluctuations on the Fe ions. Although the local interaction in this material is quite strong leading to Mott insulator behavior, the charge and spin fluctuation is still strong for such a multi-orbital system, which reduces the single particle gap from the value obtained by Hatree-Fock-type approximation (i.e. DFT+U) to about 0.1-0.2 eV.

Besides the charge fluctuation, there are also strong spin fluctuation on the Fe atoms. Configurations cf3, cf8, cf9, cf10 have total spin S=2. The total population of these configurations is P(S=2) = 0.0827. Configurations cf4, cf5, cf6, cf7 have total spin S=3, and the their total population is P(S=3) = 0.4438. Configuration cf2 has S=4, and P(S=4) = 0.247, and cf1 has S=5 with P(S=5) = 0.015. The most populated spin states in DFT+G calculations are S=3, which is smaller than the formal magnetic state S=4 in DFT+U calculations. As a result, the DFT+G calculated magnetic moments of Fe ions are smaller than those calculated by DFT+U methods.

IV. SUMMARY

We have studied the electronic structure and magnetic properties of the strongly-correlated material $La_2O_3Fe_2Se_2$, using both DFT+U and DFT+G methods. The ground states magnetic configuration obtained from DFT+U calculations are in agreement with most recent experiments.[8,9] However, DFT+U calculations greatly overestimate the band gap of the material. We then investigate electronic structure using the DFT+G method, and the results show $La_2O_3Fe_2Se_2$ is a narrow gap semiconductor, in excellent agreement with experiments. We show there are strong charge and spin fluctuations on the Fe atoms that greatly reduce the band gap and magnetic moments from the DFT+U values.

Acknowledgments

LH acknowledges the support from Chinese National Science Foundation Grant number 11374275.

[1] J.-X. Zhu, R. Yu, H. Wang, L. L. Zhao, M. D. Jones, J. Dai, E. Abrahams, E. Morosan, M. Fang, and Q. Si, Phys. Rev. Lett. **104**, 216405 (2010).
[2] D. G. Free and J. S. O. Evans, Phys. Rev. B **81**, 214433 (2010).
[3] J. M. Mayer, L. F. Schneemeyer, T. Siegrist, J. V. Waszczak, and B. v. Dover, Angew. Chem., Int. Ed. Engl. **31**, 1645 (1992).
[4] S. Landsgesell, K. Prokeš, T. Hansen, and M. Frontzek, Acta Materialia **66**, 232 (2014).
[5] M. Fiebig, J. Phys. D: Appl. Phys. **38**, R123 (2005).
[6] S.-W. Cheong and M. Mostovoy, Nature Materials **6**, 13 (2007).
[7] Y. Fuwa, T. Endo, M. Wakeshima, Y. Hinatsu, and K. Ohoyama, J. Am. Chem. Soc. **132**, 18020 (2010).
[8] M. Günther, S. Kamusella, R. Sarkar, T. Goltz, H. Luetkens, G. Pascua, S.-H. Do, K.-Y. Choi, H. D. Zhou, C. G. F. Blum, et al., Phys. Rev. B **90**, 184408 (2014).
[9] E. E. McCabe, C. Stock, E. E. Rodriguez, A. S. Wills, J. W. Taylor, and J. S. O. Evans, Phys. Rev. B **89**, 100402(R) (2014).
[10] H. Lei, E. S. Bozin, A. Llobet, V. Ivanovski, V. Koteski, J. Belosevic-Cavor, B. Cekic, and C. Petrovic, Phys. Rev. B **86**, 125122 (2012).
[11] L. L. Zhao, S. Wu, J. K. Wang, J. P. Hodges, C. Broholm, and E. Morosan, Phys. Rev. B **87**, 020406(R) (2013).
[12] J. P. Perdew, K. Burke, and M. Ernzerhof, Phys. Rev. Lett. **77**, 3865 (1996).
[13] G. Kresse and J. Hafner, Phys. Rev. B **47**, 558 (1993).
[14] G. Kresse and J. Furthmüller, Phys. Rev. B **54**, 11169 (1996).
[15] V. I. Anisimov, J. Zaanen, and O. K. Andersen, Phys. Rev. B **44**, 943 (1991).
[16] J. Bünemann, W. Weber, and F. Gebhard, Phys. Rev. B

57, 6896 (1998).
[17] X. Y. Deng, L. Wang, X. Dai, and Z. Fang, Phys. Rev. B **79**, 075114 (2009).
[18] N. Marzari and D. Vanderbilt, Phys. Rev. B **56**, 12847 (1997).
[19] I. Souza, N. Marzari, and D. Vanderbilt, Phys. Rev. B **65**, 035109 (2001).
[20] N. Marzari, A. A. Mostofi, J. R. Yates, I. Souza, and D. Vanderbilt, Rev. Mod. Phys. **84**, 1419 (2012).
[21] A. A. Mostofi, J. R. Yates, Y.-S. Lee, I. Souza, D. Vanderbilt, and N. Marzari, Comput. Phys. Commun. **178**, 685 (2008).
[22] Y. U. Wang, Z. Wang, Z. Fang, and X. Dai, Phys. Rev. B **91**, 125139 (2015).
[23] A. Georges, L. de' Medici, and J. Mravlje, Annu. Rev. Condens. Matter. Phys. **4**, 137 (2013).
[24] F. M. F. de Groot, J. C. Fuggle, B. T. Thole, and G. A. Sawatzky, Phys. Rev. B **42**, 5459 (1990).
[25] A. I. Liechtenstein, V. I. Anisimov, and J. Zaanen, Phys. Rev. B **52**, R5467 (1995).
[26] N. Lanatà, H. U. R. Strand, X. Dai, and B. Hellsing, Phys. Rev. B **85**, 035133 (2012).
[27] N. Ni, S. Jia, Q. Huang, E. Climent-Pascual, and R. J. Cava, Phys. Rev. B **83**, 224403 (2011).